Dear reviewer:

Thank you very much for your careful checking and constructive comments! We are also so appreciated for your recognition. The responses of your precious comments are as following:

Comment 1: The vertical axis of figure is not well described. It appears to be the WTCMR metric, but it is not clearly explained.

Reply: We modified Figures 5 and 9 as:

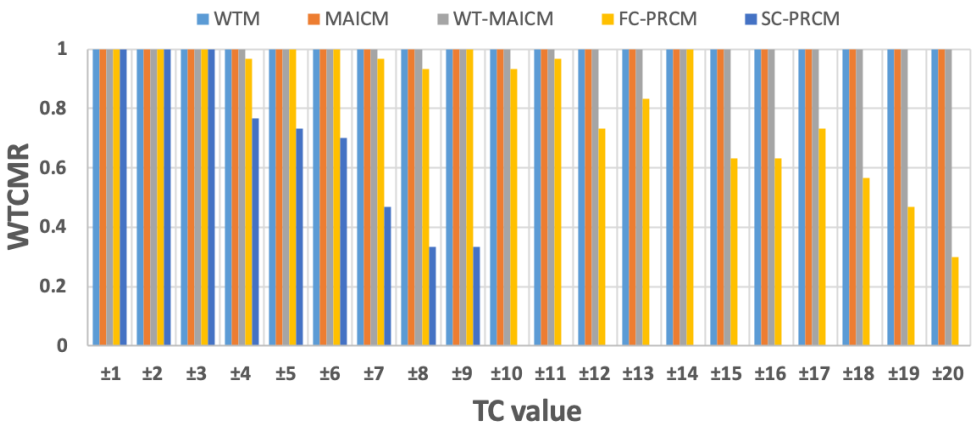


Figure 5. Well-determined topological charge (TC) measurement ratio (WTCMR) distributions of the five closed path determination methods when the TC value changes from ±1 to ±20.

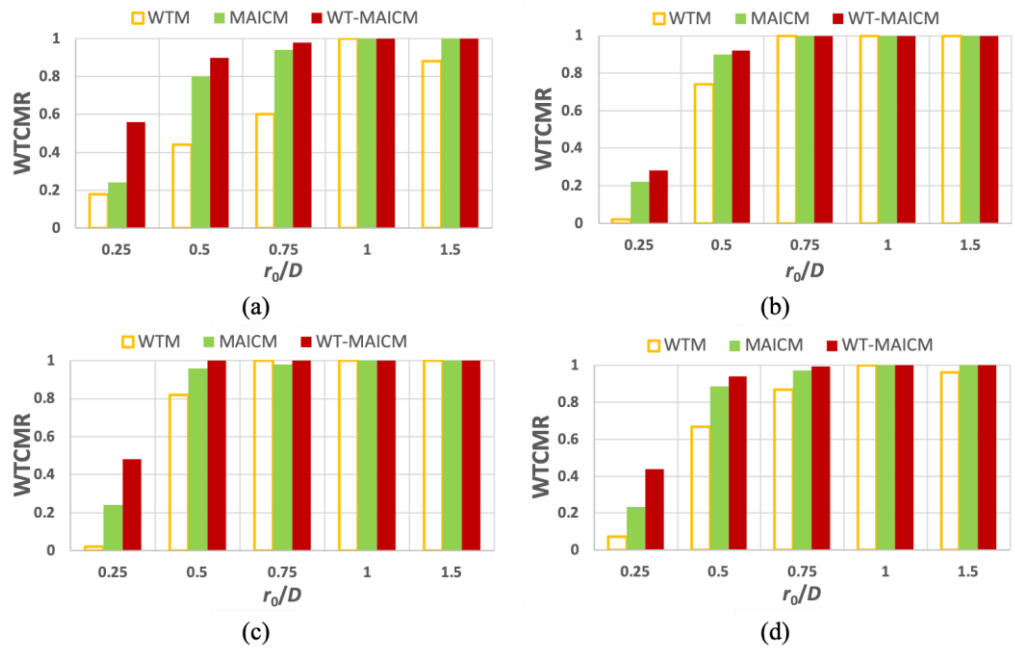


Figure 9. TC determination performance of three methods under different atmospheric turbulence conditions, where (a) is under $TC = 1$, (b) is under $TC = 5$, (c) is under $TC = 10$, and (d) is the average of (a), (b) and (c).

Comment 2: How the 15 lateral translations of the Shack Hartmann sensor was used in the method would be useful.

Reply: We added more explanation to furtherly demonstrate the usage of 15 lateral translations of the

SH-WFS at the first paragraph of the revised manuscript: "…In order to enrich the data amount as well as eliminate the randomness, for each TC value, we repeatedly recorded the Hartmanngrams at 15 different SH-WFS positions to by laterally moving the mechanical platform."

Comment 3: More information on the algorithms coded could be included in supplemental or appendix to better enable replication of the study.

Reply: Thank you for this comment. We apologize that it is not convenient for us to directly share the code of algorithms in supplemental or appendix, but we would like to share the code through personal contact by email, as suggested by Reviewer2. Correspondingly we added a statement in the beginning of the conclusion section of the revised manuscript: "In this paper, we presented an experimental comparison of five closed path determination methods for the use of GCSM to detect the TC of an OV beam. These five methods are the previously proposed MAICM and FC-PRCM and three newly proposed methods: the WTM, WT-MAICM, and SC-PRCM. These methods come from two strategies: WTM, MAICM and WT-MAICM belong to the strategy of ridge extraction, and FC-PRCM and SC-PRCM are derived from the strategy of PRC assignation. Codes for algorithms are available from authors by email."

Comment 4: How the intensity profile of the vortex beam were collected could be better explained.

Reply: We modified the diagram of the experimental setup and gave the corresponding explanation of how we recorded the intensity profile image in the revised manuscript. The modifications are as follows:

4. Experimental setup

To verify the performance of these methods of closed path determination for the GCSM, we built an experimental setup as shown in Figure 3 [24]. As shown in Figure 3, a collimated laser beam of wavelength 632.8 nm passed an aperture with a diameter of 4 mm and was incident on a liquid crystal on silicon-spatial light modulator (LCOS-SLM). The LCOS-SLM was used to transform the incident beams into the optical vortex beams as well as bring aberrations into the beam. The beam reflected back from the LCOS-SLM was converged by a lens of focal length 2 m and was split by a beam splitter into two beams. Finally, we used an SH-WFS to recorded the Hartmanngram and a complementary metal-oxide semiconductor (CMOS) camera to check and record the intensity profile of the OV beam. The LCOS-SLM was set at the front focal plane of the lens while the SH-WFS as well as the CMOS camera was both located at the back-focal plane of the lens.

The LCOS-SLM (Hamamatsu, X10468-01) was a pure phase modulator consisting of 792 × 600 pixels with a pixel size of 20 × 20 μm [31]. The SH-WFS consisted of two elements: a square grid lenslet array with a pitch size of 200 μm and focal length of 11 mm, and a high-speed intelligent vision sensor with 512 × 512 pixels and a pixel size of 20 × 20 μm [32]. The SH-WFS was mounted on a mechanical platform that could be moved along the horizontal direction. The movement was precisely controlled by a stepping motor system. The CMOS camera was with 2592 × 2048 pixels and a pixel size of 4.8 μm × 4.8 μm.

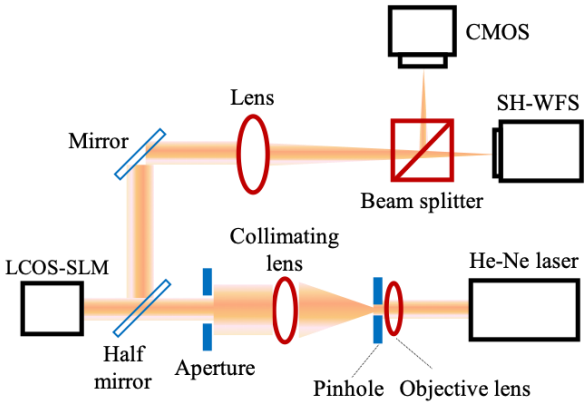


Figure 3. Schematic diagram of the experimental setup.

5. Results and discussion

5.1. Performance comparison based on aberration-free OV beams

To compare of the above five closed path determination methods, we first evaluated the performance under the aberration-free OV beam condition. In the experiments, we displayed various computer-generated holograms (CGHs) with a spiral phase structure on the LCOS-SLM to generate an OV beam with TC values ranging from ±1 to ±20. In order to enrich the data amount as well as eliminate the randomness, for each TC value, we repeatedly recorded the Hartmanngrams at 15 different SH-WFS positions by laterally moving the mechanical platform. Hence, we obtained a total of 600 Hartmanngrams (40 TC values and 15 SH-WFS positions). Figure 4 shows an example of the spiral phase pattern displayed on LCOS-SLM, and the corresponding Hartmanngram as well as intensity profile image respectively recorded by SH-WFS and CMOS camera.

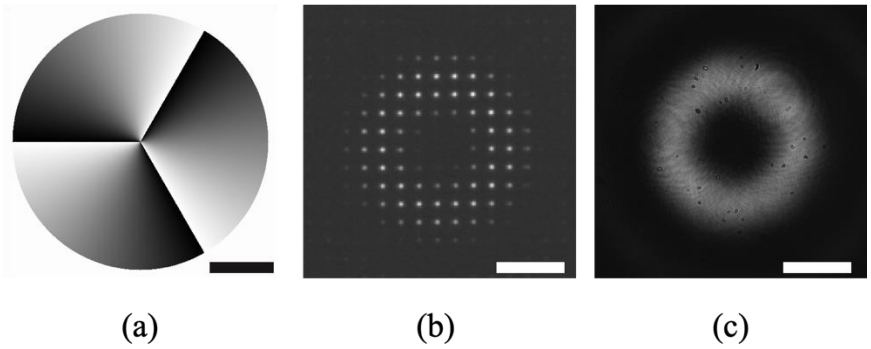


Figure 4. Example of (a) spiral phase pattern, (b) Hartmanngram, and (c) intensity profile recorded by the complementary metal-oxide semiconductor (CMOS) camera. The bar indicates 1 mm.

Comment 5: Some minor grammatical changes could help with readability.

Reply: We are sorry for our carelessness in writing. We checked our manuscript again and also submitted our paper to MDPI for further English editing. We believe the revised manuscript is better and with enough readability.